

NOVEL MICROSTRIP HAIRPINLINE NARROWBAND BANDPASS FILTER USING VIA GROUND HOLES

A. Hasan

School of Electrical and Computer Engineering
Georgia Institute of Technology
Atlanta, GA 30332, USA

A. E. Nadeem

Department of Avionics Engineering
College of Aeronautical Engineering
National University of Sciences and Technology
Risalpur, Pakistan

Abstract—In this paper, we present a novel improved hairpinline microstrip narrowband bandpass filter with via ground holes. The new filter design methodology is derived from conventional hairpinline filter design. This design methodology incorporates use of $\lambda/8$ resonators, thereby reducing the size of the filter by 35% as compared to the conventional design. An analysis is presented to show the effects of tap point height and microstrip width on fundamental parameters of filter and subsequent relationships are developed. Through use of via ground holes and a wider microstrip line for resonators, 3 dB Fractional Bandwidth (FBW) less than 2%, Insertion Loss (IL) less than 1.6 dB and Return Loss (RL) better than 40 dB is achieved with midband center frequency 1 GHz. Spurious response suppression is achieved till $3f_0$. Robustness of this design approach is demonstrated by designing filters on two more substrates having ϵ_r 2.17 and 9.2. As low as 0.48% FBW was achieved by using different substrates. The design approach is successfully tested for center frequency upto 2 GHz beyond which folding the resonator becomes practically difficult. Finally, a bandpass filter is designed with this design methodology and fabricated using FR4 substrate. S-parameter measurements show a good agreement with the simulated results.

1. INTRODUCTION

In microwave communication systems, high performance and small size bandpass filters are essentially required to enhance the system performance and to reduce the fabrication cost. Parallel coupled microstrip filters, first proposed by Cohn in 1958 have been widely used in the RF front end of microwave and wireless communication systems for decades [1]. Major advantages of this type of filter include its planar structure, insensitivity to fabrication tolerances, reproducibility, wide range of filter fractional bandwidth (FBW) (5% to 50%) and an easy design procedure [2–6]. Although parallel-coupled microstrip filter with $\lambda/2$ resonators are common elements in many microwave systems, their large size is incompatible with the systems where size is an important consideration [7]. The length of parallel coupled filter is too long and it further increases with the order of filter. To solve this problem, hairpin-line filter using folded $\lambda/2$ resonator structures were developed [8, 9]. The traditional design of the hairpin topology has the advantage of compact structure, but it has the limitation of wider bandwidth and poor skirt rate due to unavoidable coupling [10]. In addition to small size, high selectivity and narrow bandwidth; good Return Loss (RL) and low cost are desirable features of narrowband bandpass microstrip filters.

Most of the present wireless applications are below 3 GHz [11]. In this spectrum, achieving narrow FBW and high quality factor (Q) while maintaining small size and low cost is a challenging task. Using a dielectric substrate with high dielectric constant (ϵ_r) results in narrower microstrip line. However, a narrower line results in stronger input/output coupling or a smaller external quality factor (Q_e) [12]. Narrow bandwidth and high selectivity demands large Q , which can be achieved through larger gaps between coupled resonators. But increasing gap between coupled resonators directly affect the filter size.

In this paper a novel microstrip hairpinline narrowband bandpass filter using via ground holes is presented. Resonator length has been reduced to $\lambda/8$ by using via ground holes on 2nd and 4th resonator, thereby reducing the overall size to almost half of the conventional hairpinline filter. Number of via ground holes is less than half used in 5 pole Interdigital filter. Weak coupling between resonators is achieved while maintaining relatively small spacing between resonators. It gains its simplicity from the fact that no lumped component is used. FBW of 0.5% to 2.7% is achieved at 1 GHz while maintaining Insertion Loss (IL) less than 3 dB and RL better than 30 dB. For the filters with parallel coupled $\lambda/2$ resonators, a spurious passband around twice the midband frequency (f_0) is almost always excited [12]. In this design,

as in Interdigital filters, the second passband of the filter is centred at about three times the midband frequency of the desired first pass band. Design is tested on different commonly available substrates having dielectric constants 2.17, 6.08 and 9.2. Proposed filter may be designed for midband frequencies up to 2 GHz beyond which IL exceeds 3 dB and folding the resonators become difficult. Based on methods of moments, a full wave EM simulator, Agilent ADS2005A Momentum was used for this design.

2. PRIOR WORK

Microwave filter design, an active research area in microwave community has many reported innovative ideas. Inter-digital and Hairpin Filters have FBW 25% using $\lambda/4$ resonators [13]. Microstrip Pseudo-Interdigital bandpass filter has size smaller than $\lambda/4$ with IL near 1.5 dB at passband [14]. Moreover, use of an expensive substrate (LaAlO₃) with a lumped capacitor increases the complexity of design and synthesis cost. FBW of 2.07% is achieved while maintaining small size using cross coupled hairpin resonators, but passband IL of 3.8 dB and RL of 13 dB does not fulfil the requirements of receiver side bandpass filter of a wireless communication system [15, 16]. Microstrip bandpass filter using a symmetrical parallel coupled line structure achieves 3 dB FBW of 5% with passband IL 1.5 dB and RL 30 dB while maintaining size almost equal to hairpin line filter [17]. FBW of 5.5% is achieved using folded $\lambda/4$ resonators coupled through shunt inductors. In this case the filter structure has small size, however use of lumped components (shunt inductors and series capacitors) adds to the complexity of design [18]. Planar bandpass filters using single patch resonators with corner cuts achieve a FBW of 13.04% [19]. Bandpass filters with transmission zeros achieve FBW of 2% at 1 GHz, however it gives RL less than 25 dB [20]. Microstrip square ring bandpass filters by Xiao have small size but give FBW of 10% at 2 GHz [21]. Bandpass filters with triangular resonators have RL close to 20 dB [22]. FBW of 4% is achieved at 2.4 GHz with Compact Split Ring Stepped Impedance Resonators, however they have RL less than 20 dB and out of band rejection of 25 dB [23]. Square loop bandpass filters give FBW of 1.5% but have a RL of just 10 dB [24]. Bandpass filters with Isosceles Triangular Patch resonator have FBW of 9.4% with RL less than 13 dB [25]. In RF and microwave circuits, low-loss and low inductance grounds are very important to achieve good gain, noise figure (NF), IL, VSWR, and bandwidth performance. The inductance of the top pad is a very significant part of the total inductance of the via structure, and minimum via hole diameter and metallization area

is usually desirable [26].

3. NOVEL BANDPASS FILTER DESIGN

For the new filter design, design equations for parallel coupled $\lambda/2$ resonator have been used [6]. To fold the resonators, it is necessary to take into account the reduction of coupled line lengths, which reduce the coupling between the resonators [12]. The arms of each hairpin resonator function as a pair of coupled lines when closely spaced. Using full wave EM simulator, Agilent ADS 2005A, a five pole ($n = 5$) filter was designed. Chebyshev response was selected and low pass prototype parameters were calculated for passband ripple of 0.1 dB ($\varepsilon = 0.1526$) and normalized low pass cutoff frequency $\omega_c = 1$ using [27].

$$\begin{aligned} g_0 &= 1, \quad g_1 = \frac{2a_1}{\gamma} \\ g_k &= \frac{4a_{k-1}a_k}{b_{k-1}g_{k-1}}, \quad k = 2, 3 \dots n \\ g_{n+1} &= 1 \text{ for } n \text{ odd} \\ g_{n+1} &= \coth^2(\beta/4) \end{aligned}$$

where

$$\begin{aligned} a_k &= \sin \left[\frac{(2k-1)\pi}{2n} \right] \quad k = 1, 2 \dots n \\ b_k &= \gamma^2 + \sin^2 \left[\frac{k\pi}{n} \right] \quad k = 1, 2 \dots n \\ \beta &= \ln \left[\coth \left(\frac{A}{2 \times 8.686} \right) \right] \quad \gamma = \sinh \left(\frac{\beta}{2n} \right) \end{aligned}$$

where A is the pass band ripple in decibels. The relation between A and ε is given by

$$A = 10 \log (1 + \varepsilon^2)$$

Depending on the order of the filter, the termination resistance could be different from the source resistance. The bandpass design parameters Q_e is calculated using [12].

$$Q_{e1} = \frac{g_0 g_1}{FBW} \quad Q_{en} = \frac{g_n g_{n+1}}{FBW} \quad (1)$$

where Q_{e1} and Q_{en} are external quality factors of the resonator at the input and output.

Commercially available substrate of Rogers, TMM 06 with a relative dielectric constant 6.08 and thickness 1.27 mm is used for this design. Hairpin resonators line width for $50\ \Omega$ characteristic impedance is calculated to be 1.85 mm [6]. A typical separation of 2 mm is kept between the two arms and the resonator length is $\lambda/8$.

Amongst other parameters used for evaluating bandpass filter performance, RL is important. In traditional design, Z_0 (terminating impedance) is chosen equal to the desired input/output impedance and Z_r (characteristic impedance of the hairpin line) is usually kept higher than Z_0 . This results in reduced microstrip width of the hairpin resonators without much affecting the RL. However in proposed design, since high impedance is produced by the power ground plane resonance, reflections are considerably increased causing a very poor RL [28]. Simplest way to minimize reflections caused due to high impedance of ground plane is to decrease the impedance of the hairpin resonators. In order to get closer to the ideal performance, Z_r is kept equal to or lower than Z_0 . Effect of varying Z_r on input/output impedance studied during this work is also included in this paper.

ADS 2005A was used to design and simulate the filter. Filter layout is shown in Fig. 1 and the results are shown in Fig. 2 and Fig. 3.

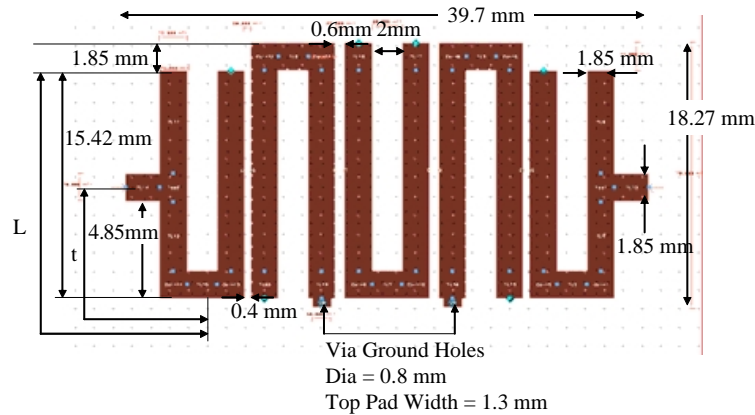


Figure 1. Layout of proposed filter designed using Rogers TMM 06 ($\epsilon_r = 6.08$).

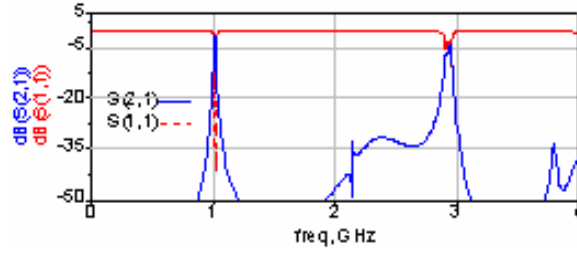


Figure 2. S-parameters results of the proposed filter designed using Rogers TMM 06 ($\epsilon_r = 6.08$).

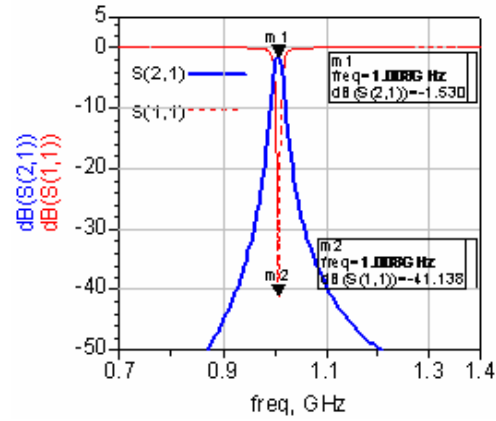


Figure 3. S-parameters results of the proposed filter designed using Rogers TMM 06 ($\epsilon_r = 6.08$).

3.1. Effect of Tap Point Location

The relationship between tap point (t) and Q_e for conventional hairpin line filter is [12]

$$t = \frac{2L}{\pi} \sin^{-1} \left(\sqrt{\frac{\pi}{2} \frac{Z_0/Z_r}{Q_e}} \right) \quad (2)$$

where t is the tap point height and L is $\lambda/8$ long. To validate the results for the proposed design, sensitivity analysis was carried out for different tapping heights and insightful results were observed. Narrower 3 dB BW renders higher Q_e which requires tap point to be lowered. The general trend observed in proposed filter is quite consistent with (2) as shown in Fig. 4.

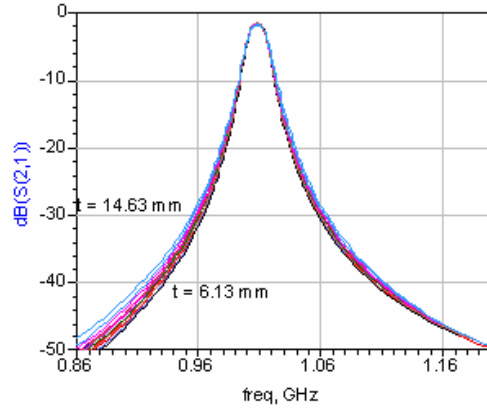


Figure 4. S_{21} plotted for different tap point locations “ t ”.

Proposed design has a FBW less than 2% which corresponds to Q_e higher than 58. For such high Q_e , tap point location calculated using (2) does not suite the geometrical dimensions of filter as shown in Fig. 5. The lowest practicable value of tap point can be calculated simply by adding microstrip resonator width; half of the microstrip tap width and one half of the separation between two arms of first/last resonator. In proposed design this value comes out to be 3.79 mm which is much more than the highest value calculated using (2): 1.84 mm. In case of proposed design, Q_e and corresponding tap point height from simulated results are plotted in Fig. 5. Proposed design provides a greater degree of freedom for placement of tap point in terms of Q_e . As t is varied from 6.13 mm to 14.63 mm, the Q_e correspondingly decreases from 66.17 (FBW 1.733%) to 62.7 (FBW 1.829%).

A second order polynomial was developed to explain the relationship between Q_e and t/L in the proposed design.

$$Q_e = -9.6514 \left(\frac{t}{L} \right)^2 + 3.352 \left(\frac{t}{L} \right) + 66.169 \quad (3)$$

In comparison if we consider the relation ship between Q_e and t calculated using (2), the relation is almost linear due to small range of t and can be expressed as

$$Q_e = -70.244t + 192.54 \quad (4)$$

For values of $t/L \geq 0.5$, the value of $\sin^2((\pi/2)(t/L))$ can be approximated as equal to t/L . Which implies that for values of

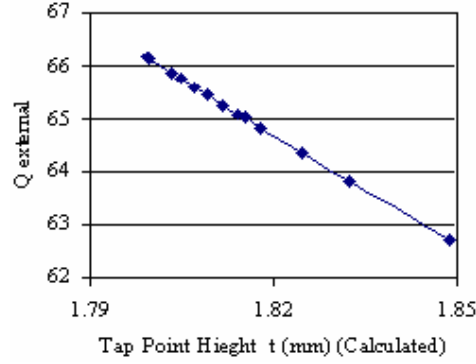


Figure 5. Q_e plotted against values of “ t ” as calculated using Eq. (2).

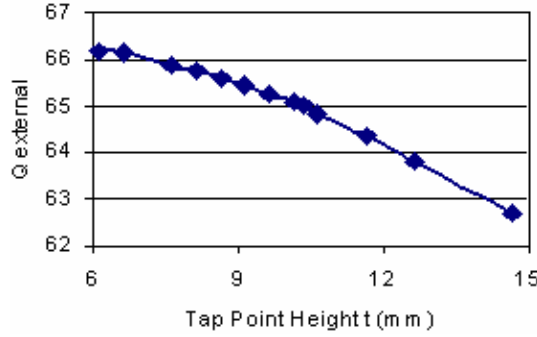


Figure 6. Q_e plotted against values of “ t ” measured through EM simulations.

$t \geq 0.5L$, (2) can be interpreted as:

$$Q_e = \frac{1}{2} \frac{Z_0}{Z_r} \left(\frac{1}{t/L} \right) \quad (5)$$

However (4) and (5) does not yield results in agreement with the results of EM Simulations. It is also important to note here that tap point placement has an observable effect on the input/output impedance of the filter. Results of sensitivity analysis for tap point in terms of S_{11} show clearly two patterns in terms of RL as shown in Fig. 7 and Fig. 8. As the tap position is lowered from 14.63 mm to 8.63 mm, RL improves, but beyond 8.63 mm till 6.13 mm, an increase in reflections is noticed. The effect of tap placement on RL and IL is displayed in Fig. 9(a) and Fig. 9(b). It is quite evident from

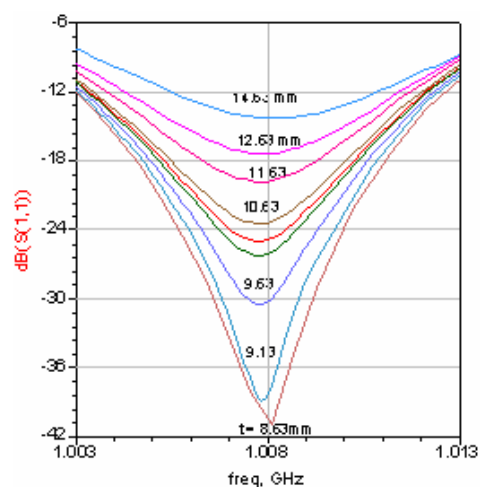


Figure 7. S_{11} plotted for different tap point locations “ t ”.

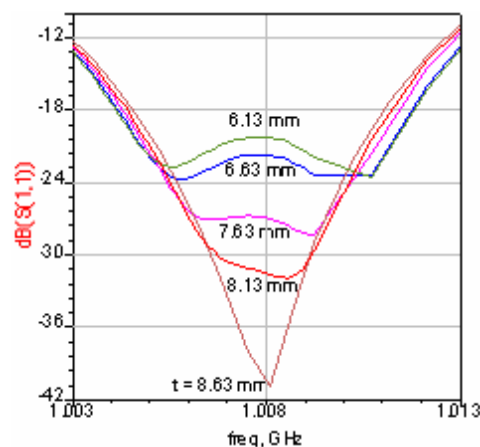


Figure 8. S_{11} plotted for different tap point locations “ t ”.

the results of the sensitivity analysis that though a lower tap point guarantees better performance in terms of Q_e , but same is not true in terms of IL and RL. In this design we are able to successfully accomplish impedance matching through adjusting the tapping point. It is interesting to note that as we lower the tapping point, input impedance reduces with considerably larger increase in the argument and vice versa. Input impedance corresponding to different tap point is tabulated in Table 1:

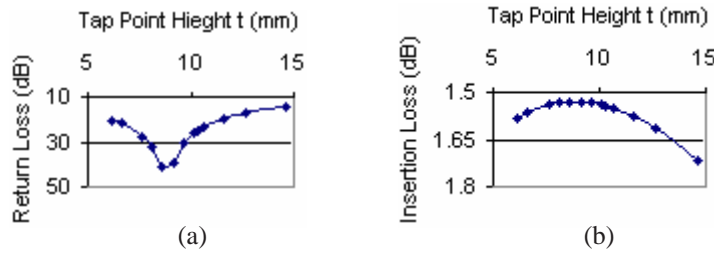


Figure 9. (a) RL plotted against “ t ”. (b) IL plotted against “ t ”.

Table 1. Input impedance Z_{in} corresponding to different Tap Point Heights (t).

S No	Tap Point (t) mm	Z_{in}
1	6.13	43.436 / -7.722
2	7.63	46.739 / -3.540
3	8.63	49.211 / -0.561
4	9.63	52.148 / 2.476
5	10.63	55.228 / 5.219
6	11.63	58.503 / 7.634
7	12.63	61.827 / 9.793
8	14.63	69.075 / 12.494

3.2. Effect of Characteristic Impedance of Hairpinline (Z_r)

Now the effect of characteristic impedance of the hairpinline resonator would be studied. The effects of microstrip width on S_{21} and S_{11} are shown in Fig. 10 and Fig. 11 respectively. These results are interpreted in terms of IL and RL in Fig. 12(a) and Fig. 12(b) respectively.

IL generally improves as we reduce the microstrip width. However, for values of microstrip resonator narrow enough to cause extremely poor RL as in case of microstrip width 1.25 mm and 1 mm, the IL also starts to degrade. The reason emanates from the basic definition of IL which mentions that in addition to attenuation, reflections are also accounted for in IL [29].

Return loss largely depends upon impedance matching, and the point where the input/output impedance matches best with the terminating impedance, RL has the largest value. RL decreases on either side of that point. Characteristic impedance of the microstrip

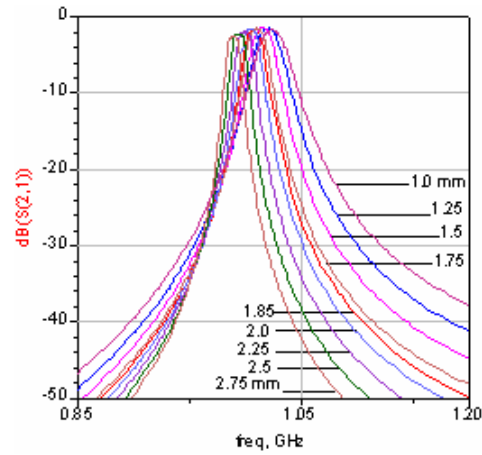


Figure 10. S_{21} plotted for microstrip width 1.0 mm, 1.25 mm, 1.50 mm, 1.75 mm, 1.85 mm, 2.0 mm, 2.25 mm, 2.5 mm & 2.75 mm.

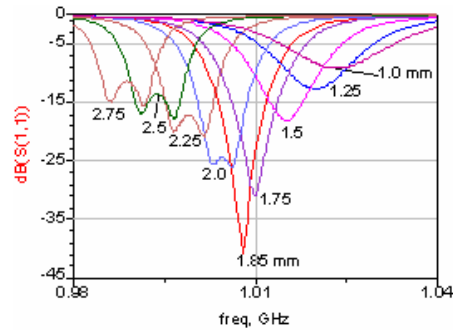


Figure 11. S_{11} plotted for microstrip width 1.0 mm, 1.25 mm, 1.50 mm, 1.75 mm, 1.85 mm, 2.0 mm, 2.25 mm, 2.5 mm & 2.75 mm.

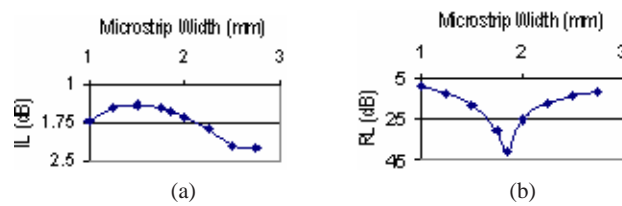


Figure 12. Effect of varying microstrip width on: (a) Insertion loss, (b) Return loss.

resonator (Z_r) has a pronounced effect on Q_e and thus on the FBW of the filter. FBW (3 dB, 20 dB and 30 dB) of the designed filter are plotted for different values of Z_r in Fig. 13.

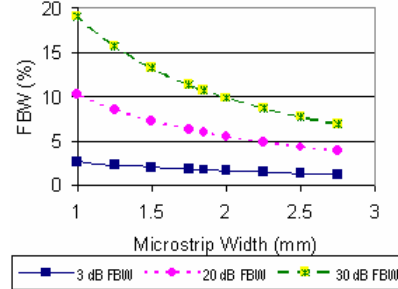


Figure 13. Effect of varying microstrip width on FBW 3 dB, 20 dB & 30 dB.

FBW decreases notably as we increase the microstrip width. Results in terms of FBW, IL and RL are tabulated for different values of microstrip widths with their corresponding Z_r in Table 2. It can be noticed that while keeping the Tap width matched to 50Ω , as the microstrip width is increased, the characteristic impedance decreases and FBW decreases. This result is not different from the design Eq. (2) reported in [12].

Rewriting (2), Q_e is related to Z_0/Z_r as shown in (6). The values of low pass prototype parameters were calculated in the beginning and do not change during the design. Meaning thereby that value of Q_e would be totally dependant on FBW. Therefore, for a design where L is given by $\lambda/8$ and tap point height is fixed, FBW can be related to the ratio Z_0/Z_r :

$$Q_e = \frac{1}{2} \left(\frac{Z_0}{Z_r} \right) \frac{1}{\sin^2 \left(\frac{\pi}{2} \frac{t}{L} \right)} \quad (6)$$

As tap point location has already been selected, therefore the value of t/L can be calculated directly. Moreover Z_0 is already selected and generally chosen to be 50Ω . Resultantly Q_e becomes dependant only on Z_r .

$$Q_e = \left[\frac{1}{2 \sin^2 \left(\frac{\pi}{2} \frac{t}{L} \right)} \right] \frac{Z_0}{Z_r} \quad (7)$$

$$\Rightarrow Q_e \propto \frac{Z_0}{Z_r} \quad (8)$$

Table 2. FBW, IL and RL for different microstrip resonator widths of proposed filter designed using TMM06 ($\epsilon_r = 6.08$).

Zr	Microstrip width (mm)	FBW %			RL (dB)	IL (dB)
		3 dB	20 dB	30 dB		
39.76	2.75	1.239	3.88	6.917	11.32	2.2576
42.17	2.5	1.358	4.327	7.731	13.52	2.209
44.9	2.25	1.495	4.868	8.718	17.146	1.887
48.06	2.0	1.642	5.502	9.882	25.343	1.642
50	1.85	1.748	5.954	10.728	41.138	1.529
56.1	1.5	2.042	7.3	13.254	18.035	1.402
61.39	1.25	2.307	8.591	15.733	12.638	1.469
68.02	1	2.631	10.244	19.025	9.092	1.725

The proportionality relation can be verified from the graph in Fig. 13; however the constant of proportionality is not the same as predicted in (7). To verify, least square fit through points was used to find out the relation ship between Q_e and Z_r using the calculated values as shown in (9):

$$Q_e = 1.095 \left(\frac{Z_0}{Z_r} \right) \quad (9)$$

However following expression was developed when the simulated data was used to relate Q_e with Z_r ,

$$Q_e = 93.471 \left(\frac{Z_0}{Z_r} \right) - 26.689 \quad (10)$$

Z_0/Z_r is plotted against Q_e calculated using (7) in Fig. 14(a) and against values of Q_e measured through EM simulations in Fig. 14(b). Using the conventional design equation, as Z_0/Z_r is varied across a range of 0.5 to 1.5, Q_e changes only from 0.8 to 1.4. However for the proposed design, Q_e changes from 42 to 95. The effect of Z_0/Z_r on Q_e in proposed design is much more pronounced as compared to the conventional design.

Z_0 is generally chosen equal to the desired characteristic impedance of the system to match the input/output impedance. Z_r can be more freely increased or decreased. Lower the Z_r , higher would be Q_e and narrower would be the bandwidth. However, increasing the resonator width would increase the overall size of the filter. Moreover

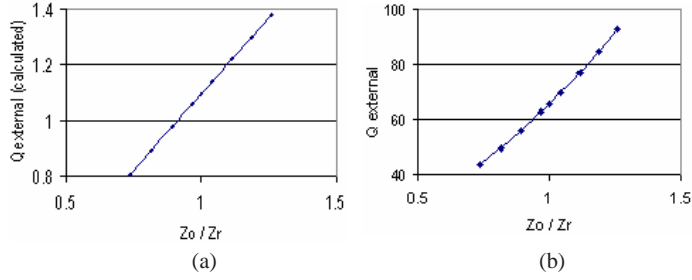


Figure 14. Z_0/Z_r plotted against Q_e (a) calculated using (10), (b) measured through EM simulations.

the increase in IL with narrow FBW can not be overlooked. In front end applications, where the signal to be received is very weak, high insertion loss cannot be afforded. In this paper, microstrip resonator width is chosen to be 1.85 mm, which gave the optimum performance. However depending upon the specific requirements of the application, different widths can be used.

Characteristic impedance of the resonator has much more pronounced effect on RL, IL and FBW in comparison to the tap point height. FBW gets narrower as Z_r is decreased. However, its effect on overall filter size can not be ignored as lower values of Z_r correspond to wider microstrip width of resonator and thus increasing the width of the filter. Though IL can be slightly improved by reducing the resonator microstrip width but this in turn results into increase in bandwidth and poor skirting. RL is largely dependant on the input/output impedance matching, and best RL is achieved for the value of Z_r which results in closest match to the value of input/output impedance.

3.3. Frequency Range of Design

In order to determine the frequency range, the proposed filter was designed at 1.5 GHz and 2 GHz. Midband centre frequency could be easily adjusted by selecting the resonator length L corresponding to $\lambda/8$ and adjusting the tapping point height. Spacing between resonator arms was set to the same typical value of 2 mm and spacing between adjacent resonators was maintained at 0.4 mm and 0.6 mm. The layout of filter at 1.5 GHz is shown in Fig. 15, and S-parameters simulated results are shown in Fig. 16.

Layout of filter at 2 GHz is shown in Fig. 17 and S-parameters simulated results are shown in Fig. 18. Performance parameters of filters at 1.5 GHz and 2 GHz are listed in Table 3.

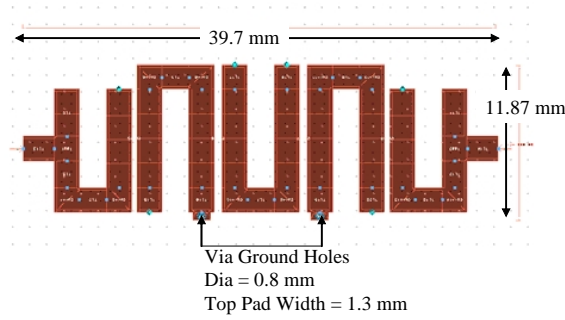


Figure 15. Layout of filter designed using Rogers TMM 06 ($\epsilon_r = 6.08$) with f_c 1.5 GHz.

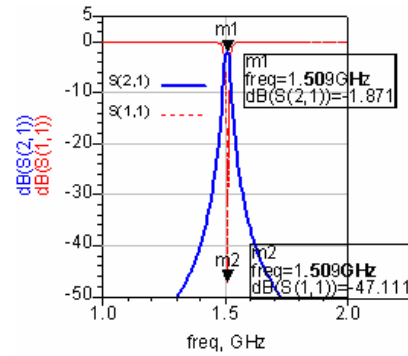


Figure 16. S-parameters results of the proposed filter designed using Rogers TMM 06 ($\epsilon_r = 6.08$).

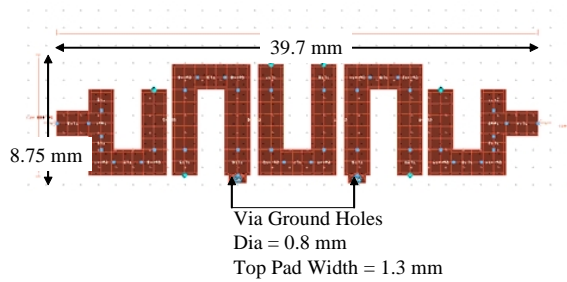


Figure 17. Layout of proposed filter designed using Rogers TMM 06 ($\epsilon_r = 6.08$) with midband centre frequency 2.0 GHz.

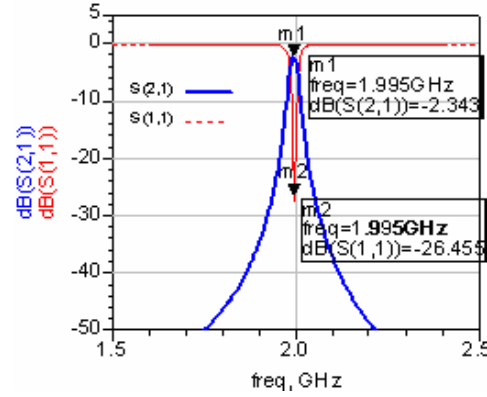


Figure 18. S-parameters results of the proposed filter designed using Rogers TMM 06 ($\epsilon_r = 6.08$) with midband centre frequency 2.0 GHz.

Table 3. Performance measures of the proposed filter designed using Rogers TMM 06 ($\epsilon_r = 6.08$) with midband centre frequency 1.5 GHz & 2.0 GHz.

Design Freq.	Area(mm ²)	FBW %			RL(dB)	IL(dB)
		3 dB	20 dB	30 dB		
1.5 GHz	471.239	1.462	5.22	9.425	47.11	1.8711
2 GHz	347.375	1.032	3.762	6.804	26.455	2.343

It was noticed that at higher frequencies, the length to width ratio of coupled microstrip lines become smaller and it becomes difficult to fold the resonator. This limitation is more pronounced in the new design for two reasons. First of all, the new design gains its compactness and size reduction through use of $\lambda/8$ resonators as compared to $\lambda/4$ resonator in conventional design. Secondly, this design requires Z_r to be equal to or lesser than the Z_0 , which results in wider microstrip resonators. To minimize the effect of this limitation, a substrate with higher ϵ_r and/or less height may be used. Overall size of filter also reduces with a high ϵ_r thin substrate as the length of the resonator is inversely proportional to the square root of ϵ_r . The dielectric thickness determines the width of the microstrip line for various impedance values. It is important to note that the relationship between the width of the microstrip and the dielectric height is not linear, therefore a decrease in dielectric height will mean a greater decrease in width of microstrip lines [6]. Though reducing the microstrip thickness would

reduce the microstrip width, but it would cause an increase in losses as well. This limitation can be addressed by using a substrate with very low loss tangent. For example, it was seen that at 2.4 GHz, if the dissipation factor is improved from 0.0023 to 0.0008, IL reduces from 3.4 dB to 1.5 dB

4. COMPARISON WITH CONVENTIONAL DESIGN

In order to compare the design with the conventional hairpinline filter, a bandpass filter is designed using the traditional design methodology with the midband centre frequency at 1 GHz [12, 30]. Rogers substrate TMM 06 is used and lowpass prototype parameters, spacing between adjacent resonators, and spacing between resonator arms is kept same as for proposed design. Microstrip resonator width is chosen to be 1 mm ($Z_r = 68 \Omega$) while the tap width is maintained at 1.85 mm. The layout of conventional hairpinline filter designed at 1 GHz is shown in the Fig. 19.

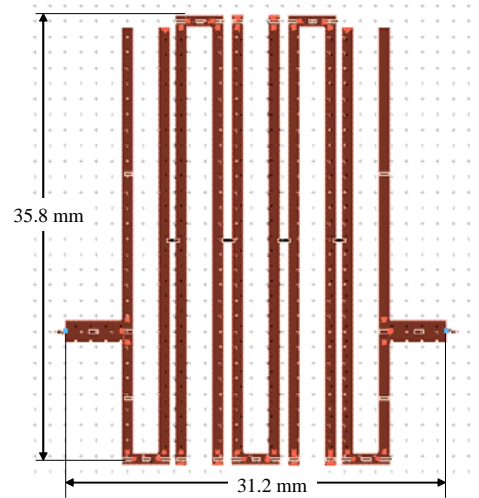


Figure 19. Layout of conventional hairpinline filter designed using Rogers TMM 06 ($\epsilon_r = 6.08$) with midband centre frequency 1.0 GHz.

EM simulation S-Parameters results of conventional hairpinline filter and proposed design are shown in Fig. 20(a) and Fig. 20(b) respectively.

In the new design, the size has been reduced by 35% and a FBW of less than 2% is achieved without increasing the spacing between coupled resonators. Though the IL is slightly increased, however the

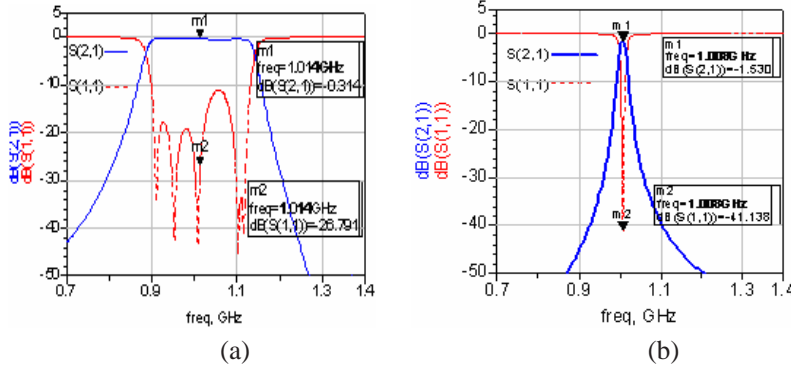


Figure 20. S-parameters results of the (a) conventional, (b) proposed filters designed.

RL is improved up to almost 40 dB. A comparison between two designs and performance parameters is tabulated in Table 4.

Table 4. Comparison of the proposed filter with conventional hairpinline filter using Rogers TMM 06 ($\epsilon_r = 6.08$) with midband centre frequency 1.0 GHz.

Design Type	Area(mm ²)	FBW %			RL(dB)	
		3 dB	20 dB	30 dB	20 dB	30 dB
Conventional	1116.96	25.034	26	0.314	33.946	40.967
Proposed	726	1.729	41.138	1.546	5.922	10.678

5. PROPOSED DESIGN ON DIFFERENT SUBSTRATES

5.1. Design Using Arlon Cuclad 217 ($\epsilon_r = 2.17$)

Using the same design technique, a bandpass filter with f_c at 1 GHz was designed using commercially available Arlons substrate CuClad217. Layout of filter is shown in Fig. 21.

The substrate has a relative dielectric constant 2.17 with dissipation factor 0.0008. As a lower dielectric constant would result in longer and wider microstrip resonators, substrate height of 0.8 mm was chosen to offset this effect. Keeping microstrip width 3.25 mm ($Z_r = 41.289 \Omega$), the 3 dB FBW thus attained is 0.481%, with IL 2.269 dB in pass band. RL greater than 30 dB is observed while out of

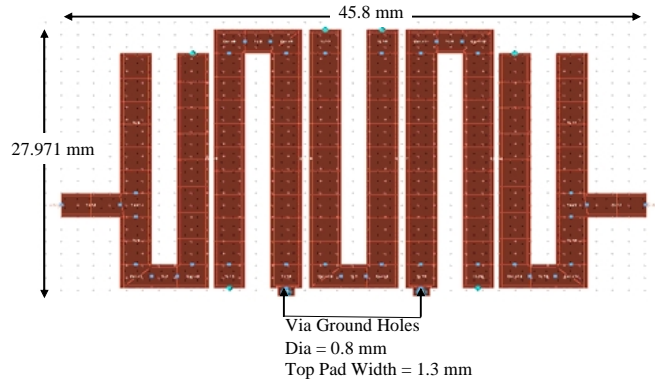


Figure 21. Layout of proposed filter designed using Arlon's CuClad 217 ($\epsilon_r = 2.17$).

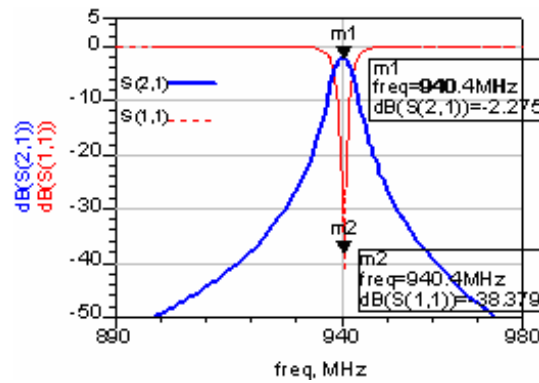


Figure 22. S-parameters results of the proposed filter designed using Arlon's CuClad 217 ($\epsilon_r = 2.17$).

band rejection is quite high as 30 dB bandwidth is less than 30 MHz. S-parameter results thus obtained are shown in Fig. 22.

It can be noticed that values of tap point height " t " calculated using (2) are not practicable as the highest tap point location thus calculated is even less than half of the microstrip width. A second order polynomial was developed to explain the relationship between Q_e and t/L in the proposed design as shown in (11). If t is calculated using (2), the tap point height varies over a very small range and the relation between Q_e and t is almost linear for that small range as shown in Fig. 23(a). However the results recorded from EM simulations are

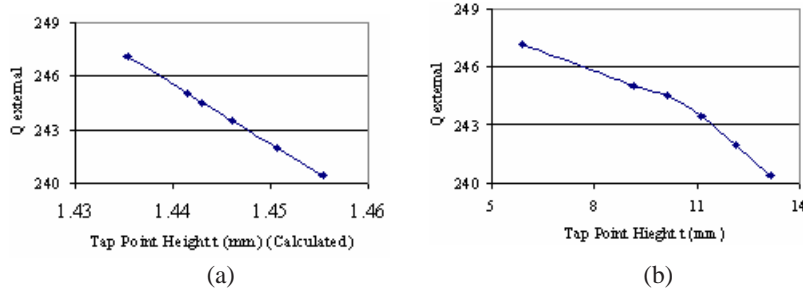


Figure 23. Q_e plotted against calculated values of “ t ” using Eq. (2). (b) Q_e plotted against values of “ t ” measured through EM simulations for proposed design.

plotted in Fig. 23(b).

$$Q_e = -0.164 \left(\frac{t}{L} \right)^2 + 23.04 \left(\frac{t}{L} \right) + 245.45 \quad (11)$$

Effect of varying “ t ” on RL was almost similar in pattern as was with the design using Rogers TMM06 and is shown in Fig. 24.

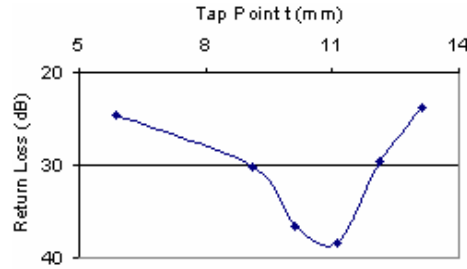


Figure 24. RL plotted against “ t ” (Tap point height).

5.2. Design Using Rogers TMM 10 ($\epsilon_r = 9.2$)

With this design technique, a bandpass filter with centre frequency at 1 GHz was designed using commercially available Rogers substrate TMM 10. The substrate has a relative dielectric constant 9.2 with dissipation factor 0.0023. Substrate height of 1.27 mm was chosen. The layout of design is shown in Fig. 25. Effects of tap point location on S_{11} are shown in Fig. 26. RL and IL as well vary with varying tap height (t) as shown in Fig. 27(a) & Fig. 27(b) respectively. S-parameter response of proposed filter designed on Rogers TMM 10 is shown in

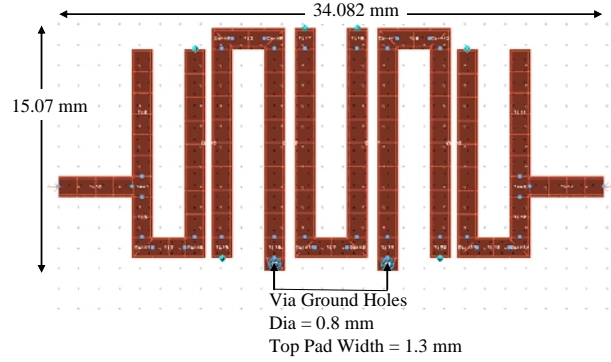


Figure 25. Layout of proposed filter designed using Rogers TMM 10 ($\epsilon_r = 9.2$).

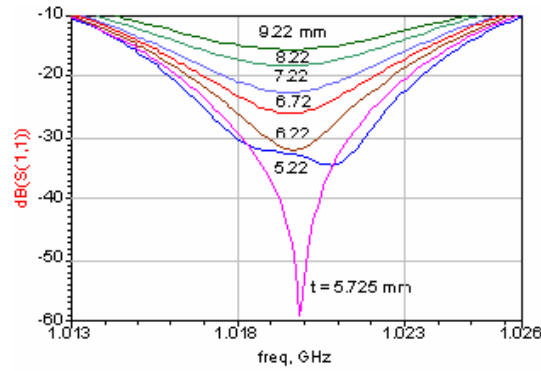


Figure 26. S_{11} plotted for different tap point locations. “ t ” as defined in Fig. 1.

Fig. 28. RL followed the same pattern as was in case of design with Rogers TMM 06 and CuClad 217.

A second order polynomial was developed to explain the relationship between Q_e and t/L in the proposed design as shown in (12).

$$Q_e = -12.68 \left(\frac{t}{L} \right)^2 + 5.2683 \left(\frac{t}{L} \right) + 53.527 \quad (12)$$

Values of t calculated using (2) are plotted against Q_e in Fig. 29(a) while the values of t obtained through EM simulations are graphed in Fig. 29(b).

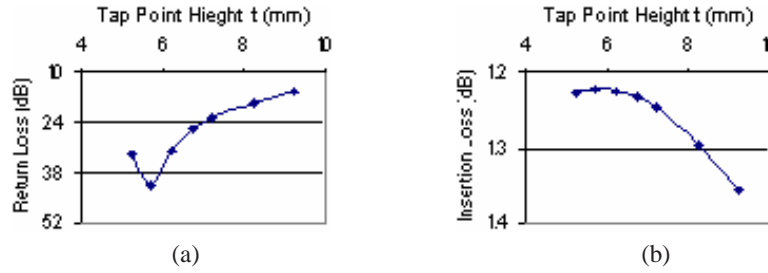


Figure 27. (a) RL plotted against “ t ”, (b) IL plotted against “ t ”.

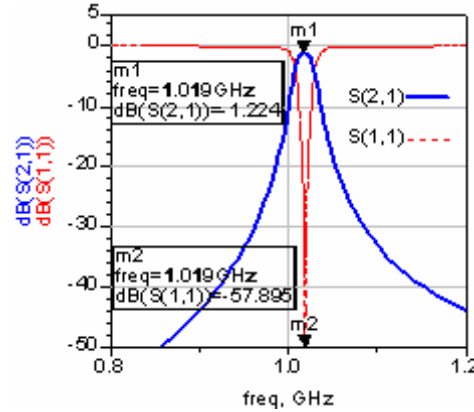


Figure 28. S-parameters results of the proposed filter designed using Rogers TMM 10 ($\epsilon_r = 9.2$).

Use of a higher dielectric constant ($\epsilon_r = 9.2$) substrate resulted in further size reduction and the overall filter size is now reduced to 514 mm^2 , which is around 20% smaller as compared to similar design using TMM 06 ($\epsilon_r = 6.08$), and 67% smaller as compared to similar design using CuClad 217 ($\epsilon_r = 2.17$). With a RL greater than 41 dB and IL of 1.224 dB in pass band, 3 dB FBW is 2.134%. 20 dB FBW of 7.135% and 30 dB FBW of 13% prove high selectivity and good out of band rejection.

6. FABRICATION AND MEASUREMENTS

Agilent ADS 2005A [30] was used for the EM simulations. Despite the reliability of the software, proposed filter was fabricated and measurements were recorded. FR4 substrate, due to its cost and

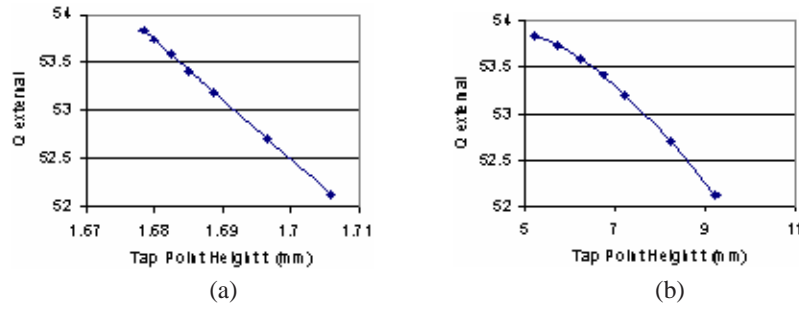


Figure 29. (a) Q_e plotted against calculated values of “ t ” (a) using (2), (b) Q_e plotted against values of “ t ” measured through EM simulations.

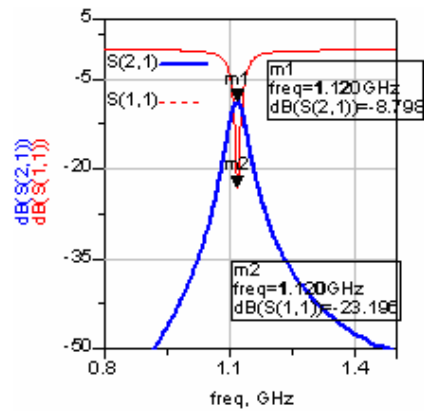


Figure 30. S-parameters results of the proposed filter designed using FR4 ($\epsilon_r = 4.34$).

availability, is one of the most commonly used laminate for microstrip structures. The biggest limitation offered by FR4 is in terms of high loss tangent ($\tan \delta = 0.02$). Such a high dissipation factor causes high insertion loss. However, for validation of design approach, close agreement between simulated and measured results was targeted. The proposed filter was designed and fabricated using FR4 substrate with dielectric constant (ϵ_r) 4.34, thickness 1.5 mm and loss tangent ($\tan \delta$) of 0.02. EM simulations for the filter were carried out and S-parameters results are shown in Fig. 30. Filter was fabricated using LPKF prototyping machine [31]. For the purpose of measurement, SMA connectors 23 SMA-50-0-51/199-NE manufactured by Huber &

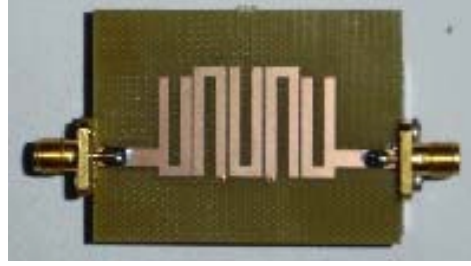


Figure 31. Snapshot of the fabricated filter.

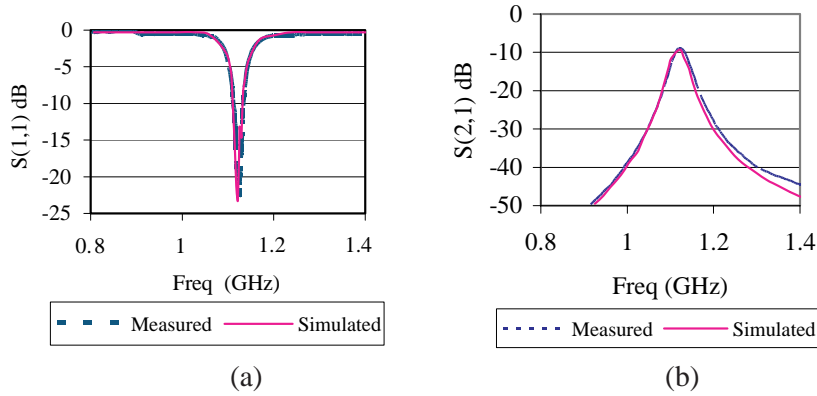


Figure 32. S-parameters measured and simulated results of the filter designed using FR4 ($\epsilon_r = 4.34$) (a) S_{11} , (b) S_{21} .

Suhner Corporation were used [32]. Snap shot of manufactured filter is shown in Fig. 31. The measured results are compared with the simulated results in Figs. 32(a) and (b) and very good agreement is found between measured and simulated results. Percent errors in f_c , IL and RL are 0.15%, 2.05% and 3.28% respectively.

7. CONCLUSION

In this paper we have presented a novel miniaturized microstrip hairpinline filter incorporating use of via ground holes. This design approach uses $\lambda/8$ resonators and thus reducing the size by 35% as compared to the conventional design. Effect of tap point height and microstrip width on filter performance measuring parameters is studied. A detailed sensitivity analysis is carried out to develop

relationships. It has been shown that the effect of microstrip width is much more pronounced as compared to tap point height on FBW, IL and RL. Desired centre frequency can be easily tuned by adjusting resonator lengths. Less than 2% FBW is achieved at 1 GHz without increasing the gap between adjacent resonators. IL in passband is less than 1.6 dB and RL is greater than 40 dB with good out of band rejection. There is no spurious response till $3f_0$. In this design methodology high Q_e can be achieved with greater flexibility in tap point location. This flexibility can be used for improving the impedance matching and thereby improving the RL. Using this design approach, narrowband bandpass filters can be designed for centre frequencies upto 2 GHz. Design robustness is demonstrated by designing filters on different substrates having ϵ_r 2.17, 6.08 and 9.2. FBW as low as 0.47% could be achieved for substrates having low dielectric constant. The design approach is validated by designing and fabricating a filter on FR4 substrate. S-parameter measurements were quite accurate with reference to simulated results.

REFERENCES

1. Cohn, S. B., "Parallel-coupled transmission-line-resonator filters," *IRE Transactions on Microwave Theory and Techniques*, Vol. MTT-6, No. 4, 223–231, April 1958.
2. Matthaei, G. L., "Design of wide band (and narrow band) bandpass microwave filters on the IL basis," *IRE Transactions on Microwave Theory and Techniques*, Vol. MTT-8, No. 11, 310–314, Nov. 1960.
3. Chang, C. Y. and T. Itoh, "A modified parallel-coupled filter structure that improves the upper stop band rejection and response symmetry," *IEEE Transactions on Microwave Theory and Techniques*, Vol. 39, No. 2, 310–314, Feb. 1991.
4. Riddle, A., "High performance parallel coupled microstrip filters," *IEEE Microwave Theory and Technology Symposium Digest*, 427–430, 1988.
5. Akhtarzad, S., T. R. Rowbotham, and P. B. Johns, "The design of coupled microstrip lines," *IEEE Transactions on Microwave Theory and Techniques*, Vol. MTT-23, No. 6, 486–492, June 1975.
6. Pozar, D. M., *Microwave Engineering*, 2nd edition, Wiley, New York, 1998.
7. Collin, R. E., *Foundations for Microwave Engineering*, 2nd edition, IEEE Press, Wiley, New York, 1992.

8. Cristal, E. G. and S. Frankel, "Hairpin-line and hybrid hairpin-line/half-wave parallel-coupled-line filters," *IEEE Transactions on Microwave Theory and Techniques*, Vol. MTT-22, No. 11, 719–728, November 1972.
9. Gysel, U. H., "New theory and design for hairpin-line filters," *IEEE Transactions on Microwave Theory and Techniques*, Vol. MTT-22, No. 5, 523–531, May 1974.
10. Singh, K., R. Ramasubramanian, and S. Pal, "Coupled microstrip filters: Simple methodologies for improved characteristics, communication systems group," *India EESOF User Group Meeting*, Nov. 17, 2005.
11. Bahl, I. J., *Lumped Elements for RF and Microwave Circuits*, Artech House, Boston, London, 2003.
12. Hong, J.-S. and M. J. Lancaster, *Microstrip Filters for RF/Microwave Applications*, Wiley, New York, 2001.
13. Wong, J. S., "Microstrip tapped line filter design," *IEEE Transactions on Microwave Theory and Techniques*, Vol. MTT-27, No. 1, 44–50, Jan. 1979.
14. Hong, J.-S. and M. J. Lancaster, "Development of new microstrip pseudo-interdigital bandpass filters," *IEEE Microwave and Guided Wave Letters*, Vol. 5, No. 8, 261–263, August 1995.
15. Hong, J.-S. and M. J. Lancaster, "Cross-coupled microstrip hairpin-resonator filters," *IEEE Transactions on Microwave Theory and Techniques*, Vol. 46, No. 1, 118–122, January 1998.
16. Gu, Q., *RF System Design of Transceivers for Wireless Communications*, Springer, 2005.
17. Jantaree, J., S. Kerdsumang, and P. Akkaraekthalin, "A microstrip bandpass filter using a symmetrical parallel coupled-line structure," *The 9th Asia Pacific Conference on Communications*, Vol. 2, 784–788, 2003.
18. Deng, P.-H., Y.-S. Lin, C.-H. Wang, and C. H. Chen, "Compact microstrip bandpass filters with good selectivity and stopband rejection," *IEEE Transactions on Microwave Theory and Techniques*, Vol. 54, No. 2, 533–539, February 2006.
19. Xiao, J.-K., S.-P. Li, and Y. Li, "Novel planar bandpass filters using single patch resonators with corner cuts," *Journal of Electromagnetic Waves and Applications*, Vol. 20, No. 11, 1481–1493, 2006.
20. Zhu, Y.-Z., Y.-J. Xie, and H. Feng, "Novel microstrip bandpass filters with transmission zeros," *Progress In Electromagnetics Research*, PIER 77, 29–41, 2007.

21. Xiao, J.-K. and Y. Li, "Novel microstrip square ring bandpass filters," *Journal of Electromagnetic Waves and Applications*, Vol. 20, No. 13, 1817–1826, 2006.
22. Zhao, L.-P., X.-W. Chen, and C.-H. Liang, "Novel design of dual-mode dual-band bandpass filter with triangular resonators," *Progress In Electromagnetics Research*, PIER 77, 417–424, 2007.
23. Xiao, J.-K., S.-W. Ma, S. Zhang, and Y. Li, "Novel compact split ring stepped impedance resonators (SIR) bandpass filters with transmission zeros," *Journal of Electromagnetic Waves and Applications*, Vol. 21, No. 3, 329–339, 2007.
24. Wang, Y. X., B.-Z. Wang, and J. Wang, "A compact square loop dual-mode bandpass filter with wide stop-band," *Progress In Electromagnetics Research*, PIER 77, 67–73, 2007.
25. Xiao, J.-K., "Novel microstrip dual-mode bandpass filter using isosceles triangular patch resonator with fractal-shaped structure," *Journal of Electromagnetic Waves and Applications*, Vol. 21, No. 10, 1341–1351, 2007.
26. Swanson, D. G., Jr., "Grounding microstrip lines with via holes," *IEEE Transactions on Microwave Theory and Techniques*, Vol. 40, No. 8, 1719–1721, August 1992.
27. Kinayman, N. and M. I. Aksun, *Modern Microwave Circuits*, Artech House, Boston, London, 2005.
28. Pak, J. S., M. Aoyagi, K. Kikuchi, and J. Kim, "Band-stop filter effect of power/ground plane on through-hole signal via in multilayer PCB," *IEICE Trans. Electron*, Vol. E89-C, No. 4, 551–559, April 2006.
29. Chueng, W. S. and F. H. Levien, *Microwave Made Simple: Principles and Applications*, Artech House Inc., Washington, 1985.
30. Agilent ADS 20005A, Momentum, Agilent Technologies, CA 94304, USA.
31. LPKF EasyContac, Operating Instructions, LPKF Laser & Electronic AG, Osteriede 7, Garbsen.
32. *Suhner Coaxial Connectors General Catalogue*, 2003/04 edition, 123.